Note RD42-3

Results from the RD-42 July '95 Beam Test at CERN

John Conway
Rutgers University

30 September 1995

Abstract

Data from the four 50-micron-pitch CVD diamond detectors tested in July at CERN reveal striking differences in performance. The signal sizes in two detectors from recently grown diamond samples, one from Norton and the other from DeBeers, do not exceed those based on an earlier Norton growth, NDF_005, tested in May. However had the Norton wafer been grown to the same thickness and had material removed its performance would probably have exceeded that of the detectors from NDF_005. Of those detectors, NDF_005_F shows an extraordinarily large increase in signal size after exposure to ^{90}Sr betas for 48 hours, while the NDF_005_B detector from the same wafer shows a much more modest increase, as does the detector from the Norton July growth.

1 Overview

In May of 1995 several CVD diamond microstrip tracking detectors were tested in a 100 GeV pion beam at CERN. Among these detectors was the first such device plated with microstrips with 50 microns pitch. The results from this detector, NDF_005_B, or simply B, described in the note RD42-2, showed a large "pump-up" of a factor of 2.5 after exposure to beta radiation from a ^{90}Sr source. Its spatial resolution of 12.8 μm represents only a slight improvement on digital resolution.

In July the B detector, along with a detector denoted F cut from the same Norton wafer, were tested along with two previously untested detectors. These were denoted D (DeBeers DB-DS1) and X (Norton July growth). The test beam setup was very nearly identical to that in May, with eight silicon reference detectors equipped with VA-1 electronics. The diamond detectors, all 50-micron pitch devices, had VA-2 readout chips.

The aims of this test included

- understanding of the large radiation pump-up effect in the B and F detectors,
- verification of the spatial resolution of the 50-micron detectors, and
- measurement of the performance of the new diamond growths from Norton and DeBeers.

Table 1.
Run Summary

run	Sir 6	Sir 7	Sir 8	events
341	D (500V)	F (300V)	B (300V)	140,000
342	-	F (300V)	B (300V)	140,000
386	D (500V)	F (300V)	X (300V)	134,000
397	-	-	B* (300V)	140,000
409	-	F* (300V)	X* (300V)	140,000
410	-	F* (300V)	X* (300V)	136,000
415	D** (500V)	-	B** (300V)	101,184
424	D** (500V)	F** (300V)	X** (300V)	140,000
425	D** (500V)	F** (300V)	X** (300V)	120,000
426	D** (500V)	F** (300V)	X** (300V)	96,600

2 Data analysis

Table 1 summarizes the data used in the analysis presented here. The raw data tapes were processed with the program TELANA, resulting in DST files of the same format used for the May data. The clusters in the silicon detectors were stored on the DST along with the full diamond plane information. After alignment, micro-DSTs containing only silicon clusters and the region in the diamond planes near the track extrapolation resulted in a factor of five reduction in size, allowing disk storage of the full data set.

3 Fiducial cuts and alignment

The alignment algorithm for the silicon remains identical to that described in note RD42-2, except that the presence of more noise hits in July necessitates changes to the hit selection. To suppress noise hits, each silicon plane must have one or two clusters. In the case of two clusters, choosing the one with larger pulse height eliminates nearly all noise hits. Further requiring each silicon plane's hit to have charge exceeding 30 ADC counts removes remaining noise hits. Each silicon plane must have, in the end, one hit. The silicon reference plane alignment converges well, and results in tracking accuracies of about 2 microns.

For the diamond, careful fiducial cuts must be made to ensure that dead and noisy channels do not bias the alignment. After a rough alignment, plots such as the one shown in figure 1 allow determination of the fiducial region. These plots show the diamond cluster position minus track position as a function of track position along the strip direction v, and versus the position perpendicular to the strip direction, in units of strip number. Dead and noisy channels are reduced by requiring the seed strip and adjacent strip rms to be in the range 1-7 ADC counts, after which the fiducial ranges in v and strip for the track extrapolation can be determined. This procedure results in alignments for the diamond planes with accuracy of a few microns.

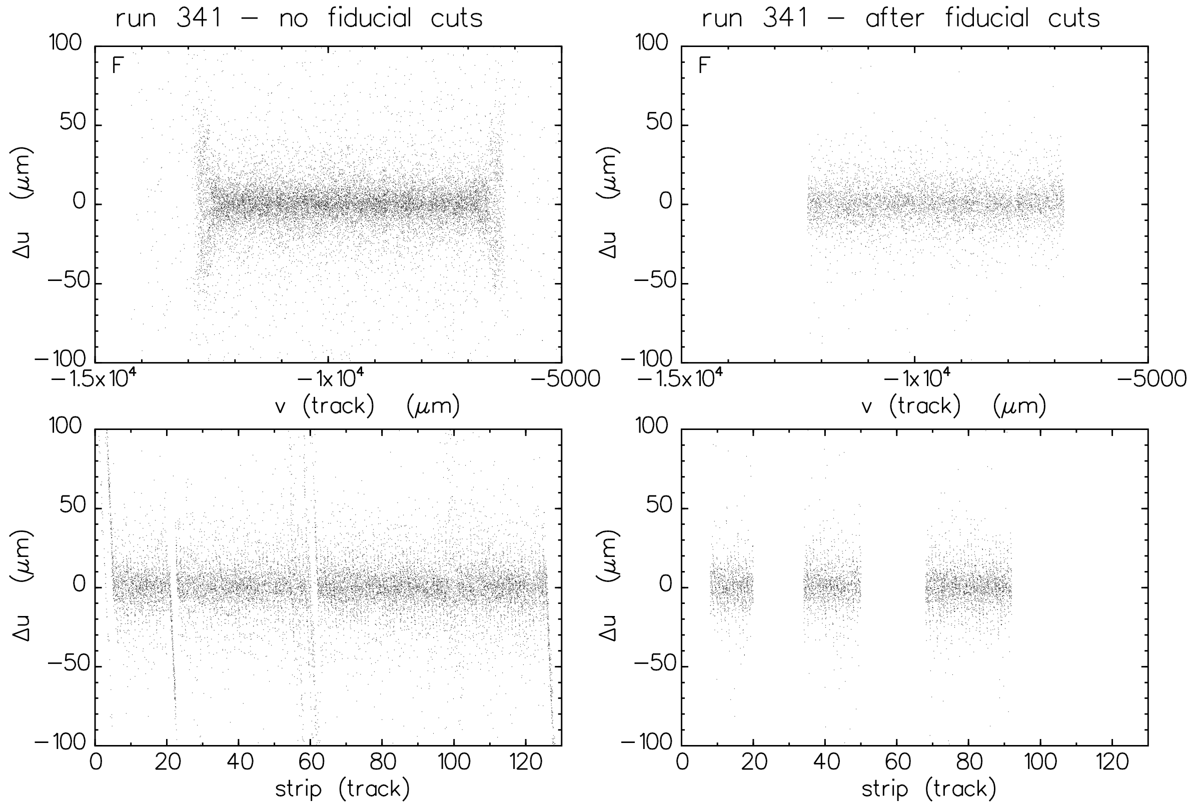

Figure 1: Hit position minus track position Δu in the F detector versus the position v of the track along the strip direction, and versus the track position in units of strip number. Left: before fiducial cuts. Right: after fiducial cuts.

4 Signal size and radiation pumping

Exposure to ionizing radiation tends to increase the size of the signal from CVD diamond detectors. One hypothesis for the mechanism underying this phenomenon is passivation of trapping sites by charges liberated by the radiation. Clear differences from sample to sample, as well as somewhat complex time dependencies, complicate the task of understanding the effect and a satisfactory quantitative model for this "radiation pump-up"has yet to appear.

In the present test data from the the D, B, F, and X detectors were recorded before exposure, after roughly one day exposure, and after roughly two days exposure to a ^{90}Sr source. The exact dose received by the detectors is not known.

The effect appears as a change in the pulse height distribution with increasing radiation dose. To make the distribution, the pulse height is calculated from the sum of the pulse heights of the strip through which the track passed and the adjacent strip with greater pulse height. Further requiring that the track in the silicon has residuals of 10 microns or less removes tracks made with incorrect hit combinations, and guarantees that a particle did pass through the diamond near the projected point. This "transparent" analysis is completely unbiased, since no information from the diamond enters the decision about whether a track is included or not.

Figures 2 through 5 show the pulse height distributions in the D, B, F, and X detectors for the carious exposure levels. The DeBeers detector D shows almost no change in pulse height, B increases by a factor of 1.5, F shows a factor of 3.5 increase, and the X detector increases by a factor of 1.8.

Table 2 summarizes these results quantitatively in terms of the average charge collected on the strips. These values require knowing the calibration factor giving the number of electrons per ADC count. These calibration constants were measured by pulsing the eletronics with a known charge and recording the response. They are accurate within 10% for a given detector. For a given detector, though, the ratio of average charge at one radiation exposure level to that at another level is accurate to about 1%.

Clearly the detectors are very different in terms of their response to exposure to ionizing radiation. The fact that the F detector shows a large pump-up factor would confirm the result from the B detector in the May test, but in fact the B detector shows only a factor of about 1.5 increase after full irradiation. The X detector, from the most recent diamond growth, shows a factor of 1.8 pump-up. This leads one to speculate that perhaps there is a chemical or physical difference between the diamond wafers from Norton, or possibly some sort of surface contamination which is affected by the strip deposition process. The fact that the DeBeers detector shows no pump-up suggests that the diamond may have started out pumped up.

Figure 4 shows the pulse height distribution for the three levels of exposure for the F detector only. There is a smooth increase in the pulse height with dose, and a plot of the values, shown in figure 6, suggests that the ultimate signal size after very long exposure might exceed 4000 electrons. The X diamond shows the same smooth increase, but with smaller signal size.

One effect observed in the May analysis is a decrease in average pulse height in the region between the strips. This effect appears in the F detector, and seems to be a smooth (not step) decrease of about 10%, independent of radiation exposure, as depicted in figure 4. The analogous plots for X and B show, however, that there is in fact no evidence for this effect in either detector. All detectors have 25-micron strips with 25-micron gaps between them.

Table 2.
Effect of Radiation Pumping on Signal Size

detector	exposure (hours)	charge[a] (ADC counts)	(electrons)
D	0	18.9	510
	24	-	-
	44	20.0	540
B	0	40.1	1083
	24	48.7	1315
	50	59.5	1607
F	0	34.5	932
	27	92.1	2487
	47	123.7	3340
X	0	25.7	694
	28	34.5	932
	48	46.2	1247

[a]The calibration used is 27 electrons/ADC count. The accuracy of the values is $\pm 10\%$ for a given diamond.

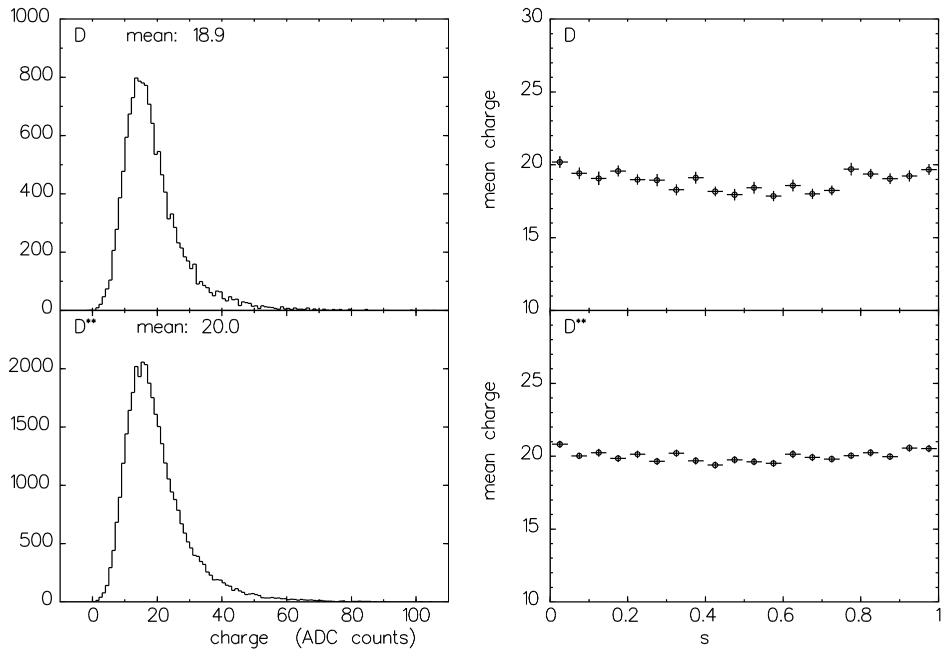

Figure 2: Pulse height distributions from a "transparent" analysis of the D detector as a function of exposure to the ^{90}Sr source (left), and mean charge as a function of the fractional strip position of the track for each exposure level (right).

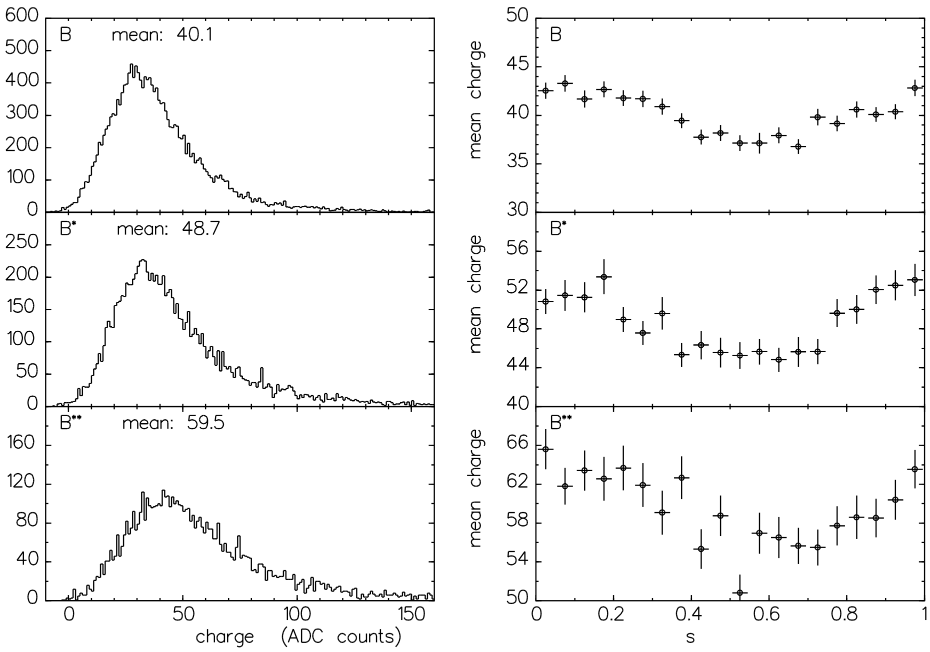

Figure 3: Pulse height distributions from a "transparent" analysis of the B detector as a function of exposure to the ^{90}Sr source (left), and mean charge as a function of the fractional strip position of the track for each exposure level (right).

5 Spatial resolution

Ultimately we seek a detector with as good spatial resolution as possible. In fact the silicon detectors used as reference planes in this analysis represent the state of the art in that parameter, with spatial resolution of 4 μm, very near the limit due to the electronic noise. In the May test the B detector had a resolution of about 13 μm, only slightly better than the digital resolution of 14.4 μm.

In the July test as well, this is roughly the resolution observed. Concentrating on the F detector, since it gave the largest signal, figure 7 shows the distribution of Δu, the hit position minus track position, for the three radiation exposure levels. As the dose increases the distributions become more gaussian, ending in a distribution with a width of 14 μm at the highest exposure. The source the non-gaussian nature of the distributions can be seen by examining the right-hand plots in the figure, which display Δu as a function of the fractional strip position of the track. When the track passes through the center of the strip, and especially for smaller charge (signal-to-noise), fluctuations in the adjacent strips bias the hit position.

This is at least in part an artifact of using a two-strip algorithm to determine the position: when the track passes through the center of a strip (s near 0 or 1) then fluctuations can determine which strip is chosen as the adjacent one. However, there is another effect which plays a role, at least in the case of the F detector.

Figure 9 shows the correlation in pulse heights of the adjacent strips with the pulse height in the center strip, using the transparent analysis of the fully-pumped F detector. The plot shows that as the center strip pulse height increases, the adjacent strip pulse heights tend to

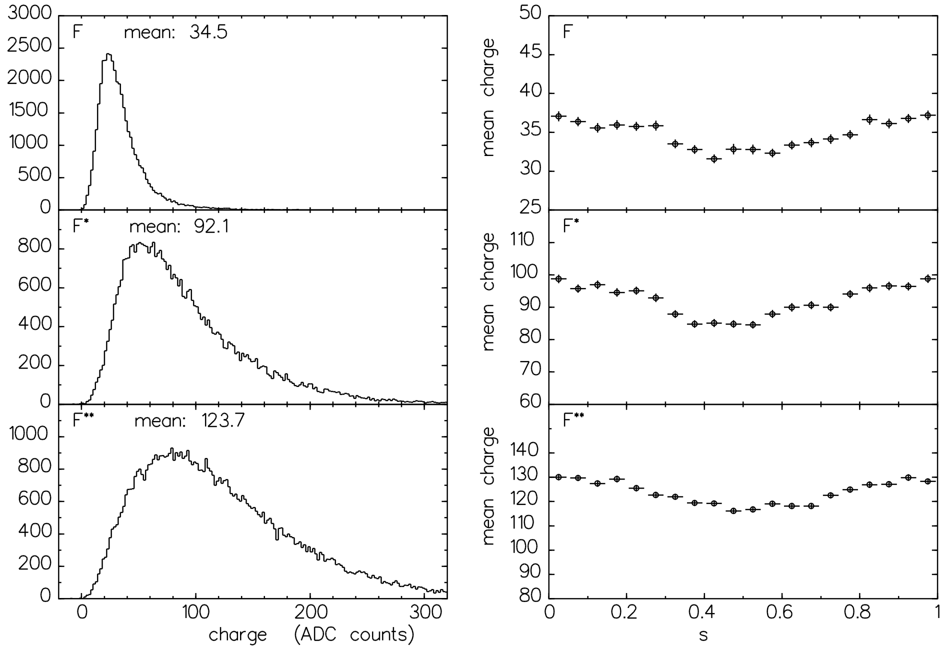

Figure 4: Pulse height distributions from a "transparent" analysis of the F detector as a function of exposure to the ^{90}Sr source (left), and mean charge as a function of the fractional strip position of the track for each exposure level (right).

go negative. This effect, possibly due to electronic cross-talk, causes the diagonal "stripes" in the plot of Δu versus the fractional strip position of the track. Plotting this correlation for those clusters with large central strip pulse height and negative adjacent strip pulse height illustrates this, as shown in figure 10.

Does this effect appear in the other detectors? Figure 11 shows the correlation of adjacent strip pulse height with central strip pulse height for the B and X detectors, after pumping. The B detector appears to display some of the tendency that F does, with the adjacent strip not showing strong positive correlation with the central strip. In the X detector, however, there is a strong positive correlation, and so one is led to question whether there are "stripes" in the plot of Δu versus fractional strip position.

Figure 8 shows these distributions, which are quite different from those in the case of th F detector. In the case of the F detector the "stripes" are buried in a broad background, whereas in the X detector there is essentially one "stripe," wrapping around in strip position space. The furthest extension of the strip does not correspond to negative-going adjacent strips, since in the case of the X detector this does not happen. The positive correlation between the center and adjacent strips, in fact, results from the fact that in the X detector the cluster width is much larger than that in the F and B detectors.

Since there is "stong" charge sharing in the X detector due to the large cluster charge width, the distribution of $\eta \equiv q_R/(q_L + q_R)$ is not flat. Since the position algorithm used here is a simple weighted average of the highest two strips, a non-flat eta distribution leads to a bias near the center of the strips. The "eta deconvolution" algorithm described in the note RD42-2 can remove this bias. Figure 12 shows the correlation of Δu with s, and the Δu distributions,

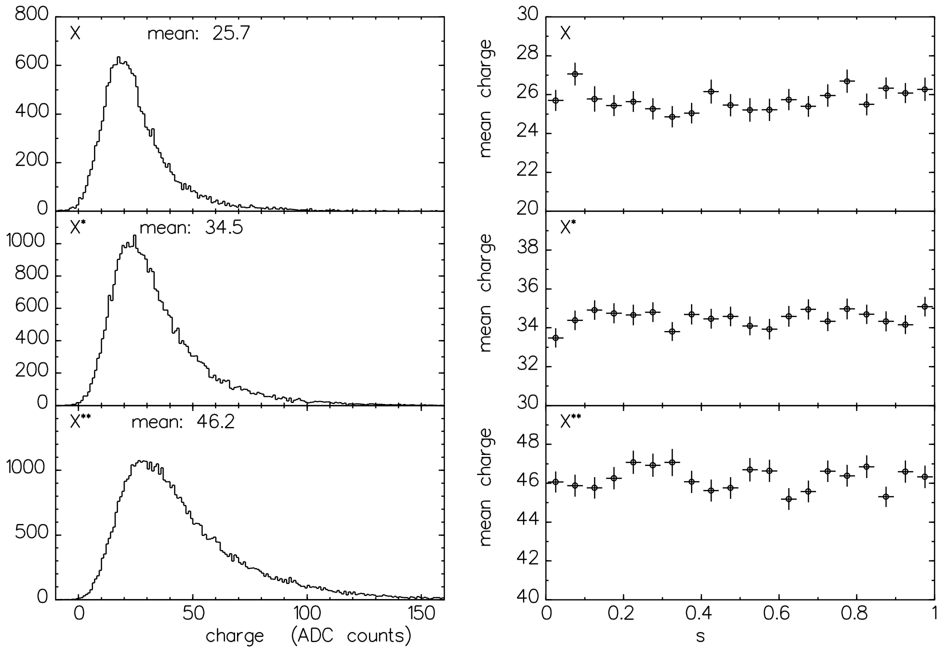

Figure 5: Pulse height distributions from a "transparent" analysis of the X detector as a function of exposure to the ^{90}Sr source (left), and mean charge as a function of the fractional strip position of the track for each exposure level (right).

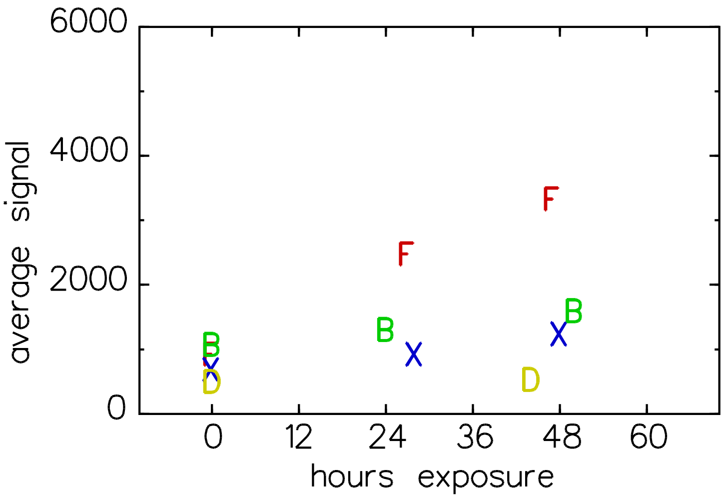

Figure 6: Average charge collected as a function of exposure time for the three Norton detectors.

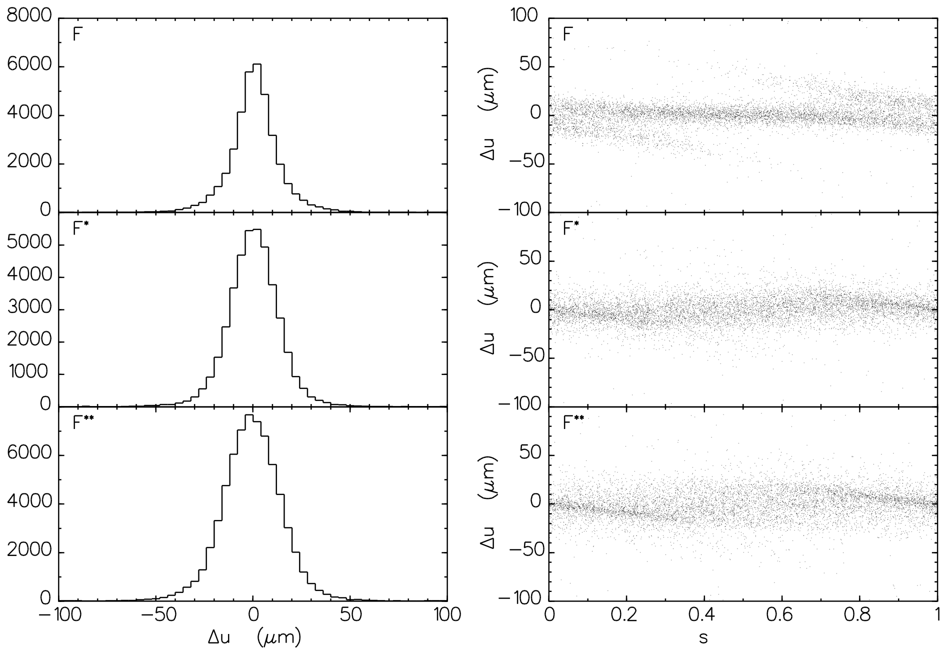

Figure 7: Distribution of Δu, hit position minus track position, (left) and Δu versus fractional strip position of track (right) for the three exposure levels in the F detector.

before and after correcting for the non-flat η distribution. This correction gives the fractional strip position of the diamond hit as the fraction of the integral of the eta distribution up to the measured eta. As the figure shows, the correction removes the "stripes" and improves somewhat the spatial resolution.

6 Discussion and Conclusions

We have measured the performance of four CVD diamond microstrip detectors in a beam test. Three of the detectors, B, F, and X, came from diamond film from Norton, and the fourth, D, came from diamond film manufactured by DeBeers. Of the three Norton detectors, B and F came from the edge of the same thick wafer, grown in early 1995, and X came from a thinner wafer grown in July. The B detector was tested in the May beam test.

One can first compare the result of the B detector with the result obtained in the May test. As seen in the note RD42-2, the B detector in the unpumped state had an initial mean charge of 1083 e^-. In the July test the B detector started with a mean charge of 1215 e^-, about 12% larger. This difference, though accounted for by the uncertainty on the calibration, could also reflect the effect of processing the detector between the tests.

Do the signals from detectors made from the same diamond agree? In the unpumped state, the F detector gives 932 e^- signal, about 15% less than the B detector. Again, the calibration might account for this.

The X detector from the more recent Norton growth shows a smaller unpumped mean charge, 694 e^-, but as noted it was not grown to the same thickness as the NDF_005 wafer. On the other hand, it was operated at 300 V, as were the thicker B and F detectors, further

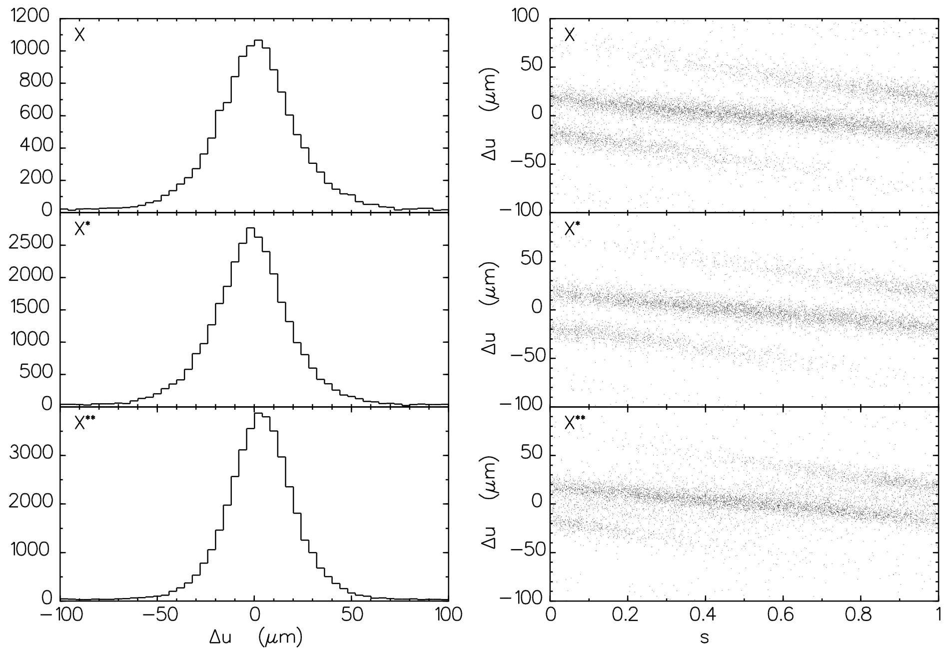

Figure 8: Distribution of Δu, hit position minus track position, (left) and Δu versus fractional strip position of track (right) for the three exposure levels in the X detector.

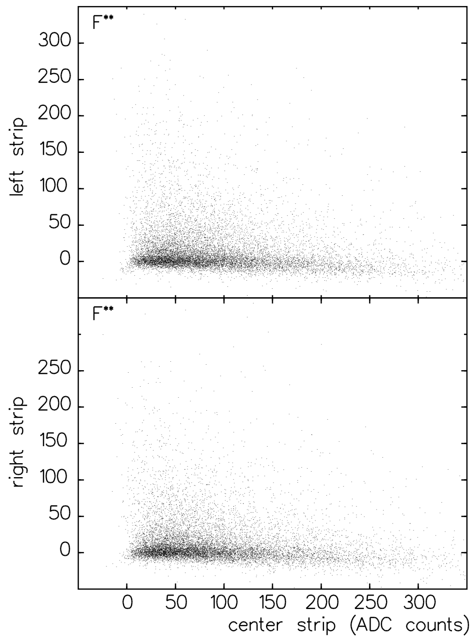

Figure 9: Correlation between pulse heights in center strip and left strip (top plot) and right strip (bottom plot) for the fully-pumped F detector.

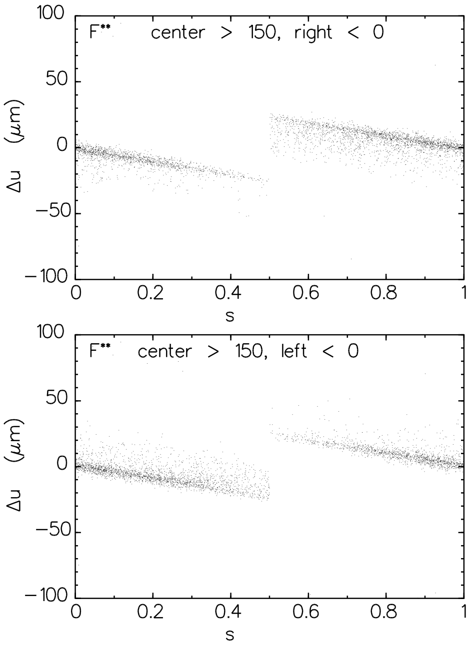

Figure 10: Distribution of Δu versus s for clusters in the fully pumped F detector haveing large central strip pulse height and negative adjacent strip pulse heights.

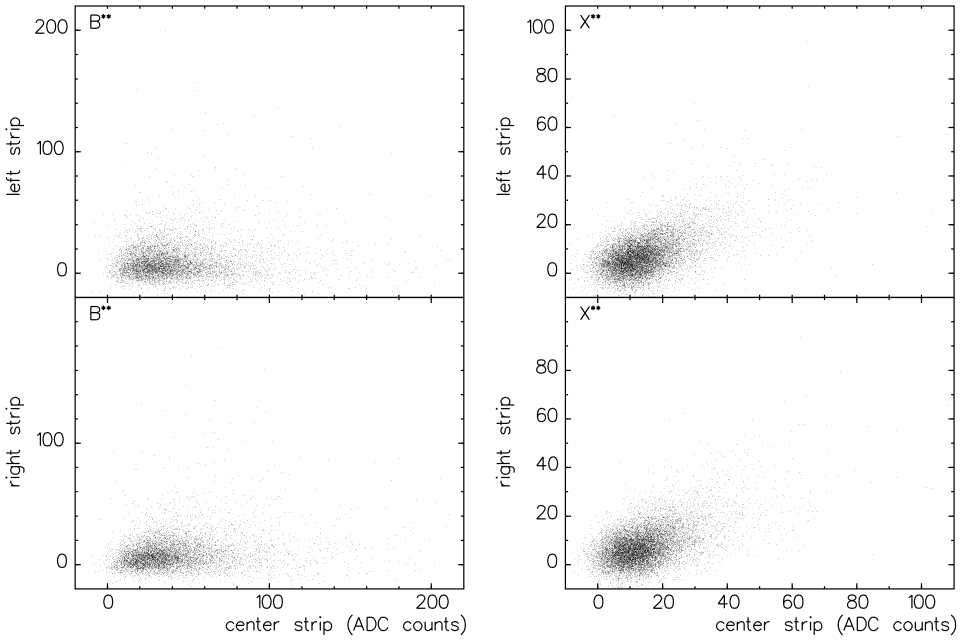

Figure 11: Correlation between pulse heights in center strip and left strip (top plot) and right strip (bottom plot) for the fully-pumped B and X detectors.

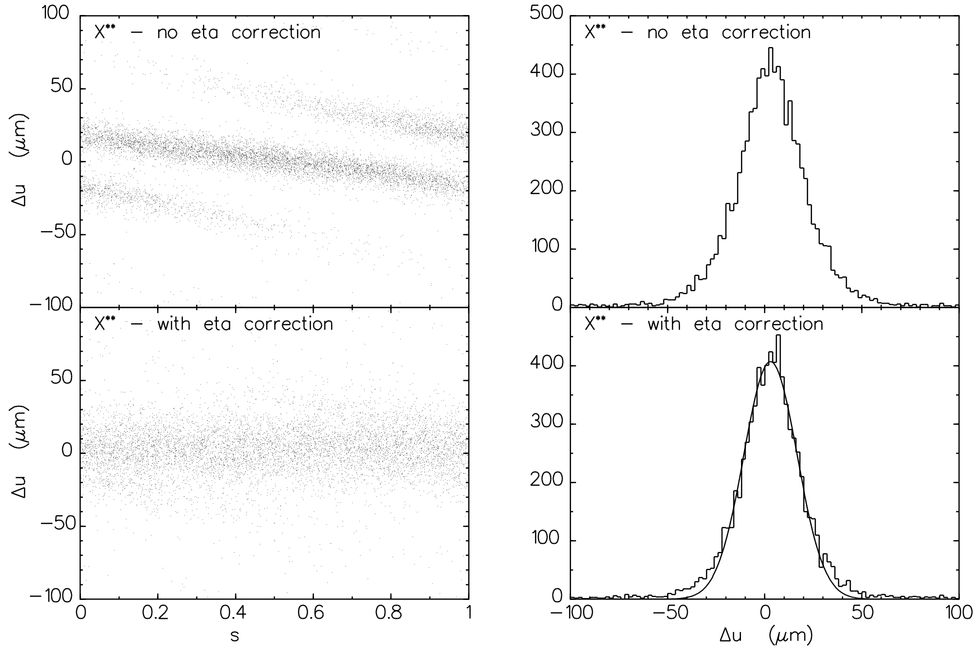

Figure 12: Correlation between Δu and fractional strip position s before and after correction for non-flat eta distribution (left), and Δu distributions for samples (right). The width of the gaussian fit to the region $|\Delta u| < 25$ μm drawn on the corrected distribution is 13.7 μm.

complicating direct comparison of the results. Had the X wafer been grown thicker and had material removed, it would have displayed roughly a factor of two larger signal. This is comparable to the signal from F or B, especially if these detectors had been operated at the same electric field.

Even if the mean charge of the detectors started out roughly the same they show a gross discrepancy in the effect of radiation exposure. The F detector signal increases by a factor of 3.5, far larger than any such increase observed on the bench, and far larger than the factor of 1.8 increase in the B detector. But the B detector also showed a factor of 2.5 increase in the May test. The plot in figure 6 clearly shows that even after 48 hours exposure the mean charge is still increasing. Thus for the B detector care must be taken in comparing the results.

The F detector displays a marked tendency for the adjacent channel pulse height to be near zero, and to drop below zero when the central strip pulse height is large. This phenomenon is amplified by pumping, which drives the tail of the pulse height distribution up. The B detector shows a similar effect, but since it has generally smaller pulse height, the effect is not as pronounced.

The X detector, on the other hand, shows a large positive correlation between the pulse height on the adjacent and central strips, in marked contrast with the NDF_005 detectors. Stated another way, the charge spreading among the strips is a great deal larger for the X detector, which also implies that the two-strip algorithm underestimates the total charge in the cluster. This raises the question whether this is a physical attribute of the diamond, or an effect related to the readout electronics.

These effects have a direct influence on the position resolution of the detectors. All of the detectors have resolution near 15-18 μm, but with non-gaussian shapes. The reason for the non-gaussian shapes appears in the plots of Δu versus fractional strip position. Ideally one would like this plot to show no correlation, but "stripes" in these plots come from the non-flat distribution of η. This correlation can be removed by correcting for this non-flatness, with a only minor improvement to spatial resolution.

Future beam tests can address the questions raised by these results:

- Are the B and F detectors equivalent in performance? Or did processing variations affect the detectors?
- Is the anomalously large pump-up with radiation exposure due to contamination in the NDF_005 diamond? Does the excess signal come from a fast or slow component?
- What causes the adjacent channel pulse heights in the B and F detectors to tend to negative values for large values of the central strip pulse height? Is it the electronics or the physics of the detector?
- How high can we "pump" the detectors' signals with radiation?

The answers to these questions will require

- careful measurement of the calibration of the electronics,
- meaurement of the integration-time-dependence of the signals for the detectors before, during, and after pumping, and
- careful, calibrated exposure to as intense a radioactive source as possible.

Acknowledgements

This document represents not only my work but the enormous effort of the members of RD42 who made the beam test happen, and made it a success. I thank them all for their dedication to this project, and for the great intellectual stimulation they have given me.